40-mm Bore Dipole Cross-Section
Using Cable Made of 1-mm-Diameter Nb_3Sn Strand

V. V. Kashikhin, I. Terechkine

The goal of this note is to put together all essential data needed to make a choice from several 40-mm bore dipole cross-sections that use 28-strand Rutherford-type cable made of 1-mm diameter Nb_3Sn strands. These data were obtained during the search for an optimal dipole cross-section of the First High Field Dipole Model to be built at FNAL. Other notes [1-4] discuss 45- and 50-mm bore dipole cross-sections using the same type of cable and 40-mm cross-section built with the use of 38-strand cable made of 0.8-mm diameter strands [5].

Cable parameters taken as a base for optimization are presented in the Table 1 below. Sample cable strand was made by Intermagnetic General Corporation (IGC) according to FNAL specification #5520-ES-362049. The method used for the strand production was internal-tin procedure. Cable was made at LBNL in accordance with the drawing provided by FNAL (see Fig. 1).

Table 1

Cable width (mm)	14.235
Cable thickness (bare) - narrow side (mm)	1.6904
Cable thickness (bare) - thick side (mm)	1.9164
Number of strands	28
Strand diameter (mm)	1.00
Cabling angle (deg.)	14.5
Cu/SC ratio	0.85
Critical current density at 11 T & 4.2 K (A/mm^2)	2427
Critical current density at 12 T & 4.2 K (A/mm^2)	1886
Critical current density at 13 T & 4.2 K (A/mm^2)	1435
Insulation thickness - azimuthal (mm)	0.12
Insulation thickness - radial (mm)	0.13

Wire critical current was measured at FNAL, and results have been reported in [6]. Although measured critical current density was slightly below the specified level due to cabling degradation, this (specified) level was taken as a reference for the cross-section optimization in a hope that wire supplier (IGC) will improve wire parameters in future.

Cable insulation thickness was chosen based on measurements made for S2 glass sleeve [7]. It depends on nominal sleeve thickness, cable cross-section perimeter, cable internal structure, applied pressure, and heat treatment history. There were no direct insulation thickness measurements made for FNAL HFD cable, but this thickness was measured with the use of KEK Nb_3Sn cable (12.2 mm width) and with Nb-Ti LHC quadrupole inner cable (15.3 mm width). Taking into the account that possible insulation material can be ceramic composite (decision pending), 0.12 mm azimuthal insulation thickness was chosen, which corresponds to about 1200 PSI (8.5 MPa) of pressure for KEK cable. Radial insulation thickness was chosen to be 0.13 mm (no pressure applied).

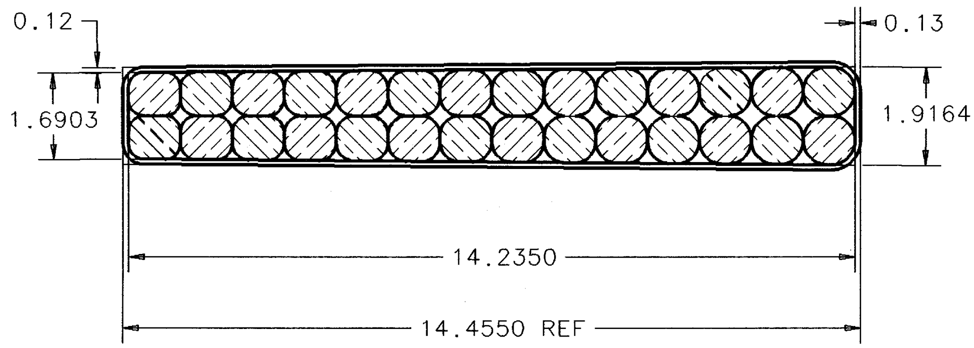

Fig. 1 HFD Insulated Cable

After cable configuration is defined, dipole cross-section can be generated and optimized using ROXIE magnet design and optimization program [8].

To have a chance to find a better cross-section, several attempts were made independently. Criteria of choice to consider were field quality, efficiency, and cable block arrangement from the viewpoint of compliance to coil winding procedure. Only two-layer designs were considered. Because the same cable data were used for all the attempts, global dipole cross-section layout did not change much. The same ground insulation thickness was used; it resulted in the same radii of internal and external layers. Ground insulation thickness was chosen consisting of two layers of 9-mill (0.23 mm) of S2 glass cloth or tape. Sketch in Fig. 2 gives an idea of the dipole coil cross-section.

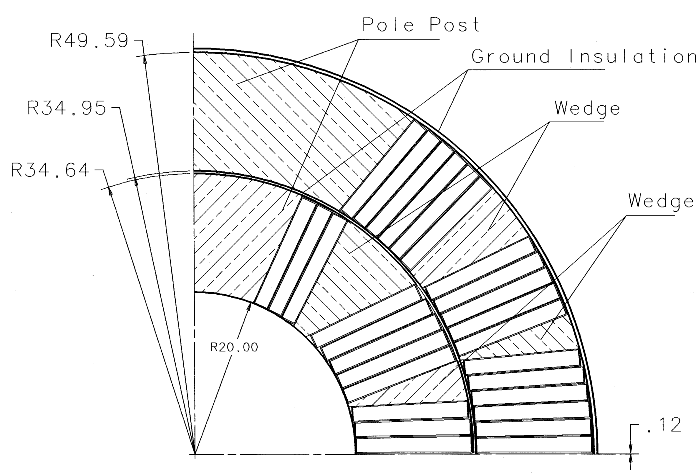

Fig. 2 HFD Cross-Section

Inner radius of iron yoke was chosen equal to 60 mm for all the cases. Linear magnetic properties with μ = 1000 were used for calculations.

Three cases were chosen to be presented in this note. In the case shown on the picture in the Fig. 2, midplane insulation was equal to 0.25 mm; a possibility to change this thickness was not included into the optimization problem. Other cases shown below (figures 4 and 5) have used this option to improve harmonic content. All cases provide reasonably good field quality and have well defined cable blocks. Pole width is 15.25 mm for case #1, 14.76 for case #2, and 15.27 for case #3. Cable winding test has been made that did not show any big problems with winding the cable around a pole with this thickness. Figures 3 to 5 show ROXIE-generated and -optimized cross-sections with field quality diagram. Table 2 summarizes harmonic content for the three designs and gives such global parameters as number of turns, maximum achievable central field (without taking into the account cable degradation) and corresponding cable current, stored energy at maximum current, inductance, and magnet efficiency.

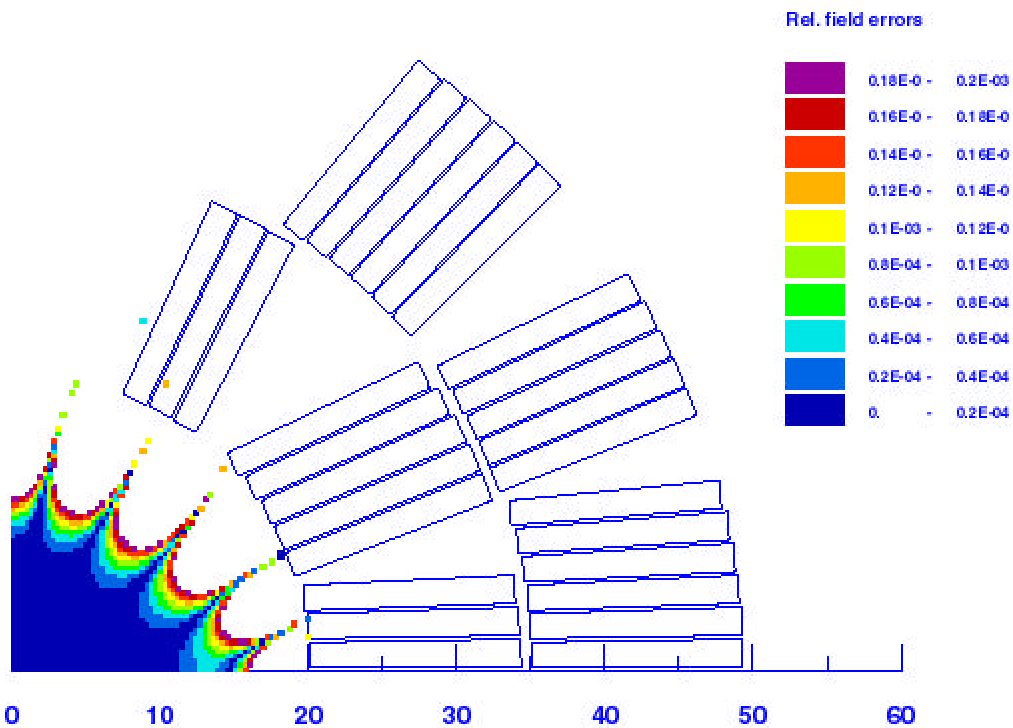

Fig.3 Field Quality Diagram. Cross-Section #1

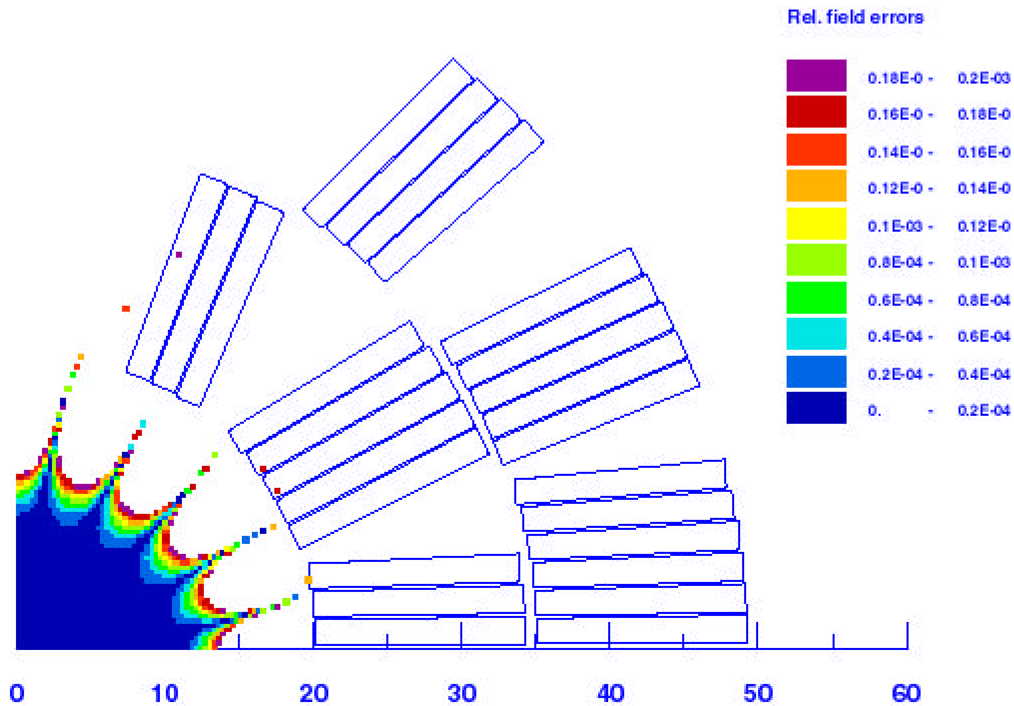

Fig.4 Field Quality Diagram. Cross-Section #2

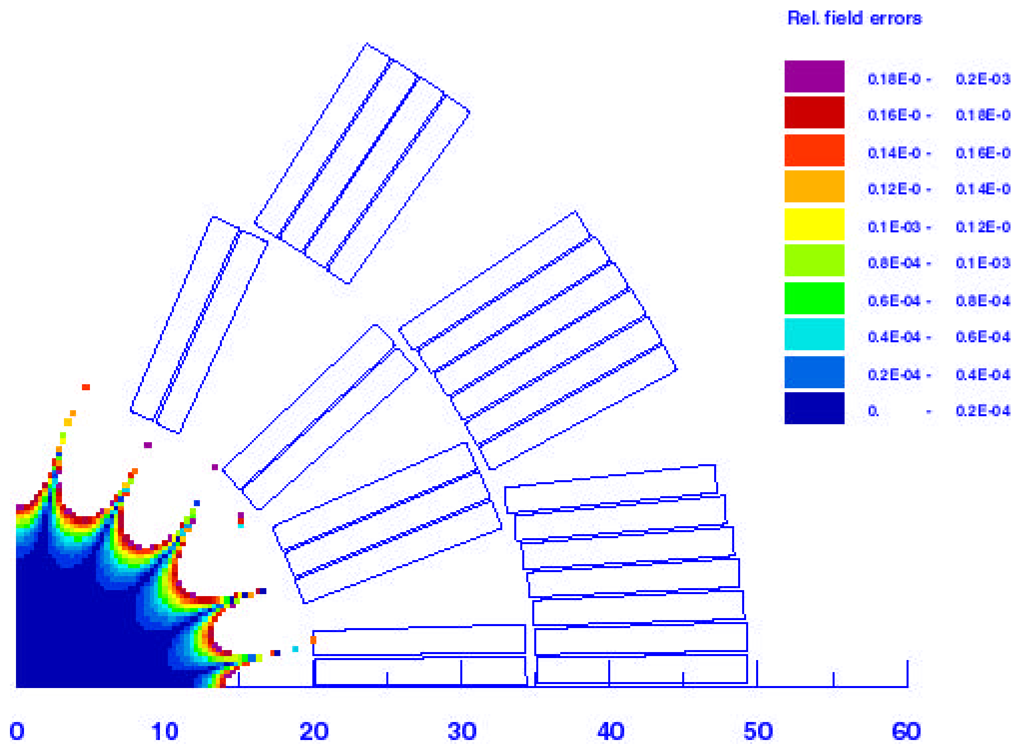

Fig.5 Field Quality Diagram. Cross-Section #3

Table 2

	#1	#2	#3
Number of turns	56	52	52
Central field at quench (T)	12.585	12.462	12.280
Quench Current (A)	17455.7	18394	18692
NI/B (A/T)	77673.9	76751.6	79154.7
Stored Energy (kJ/m)	295.55	283.21	292.00
Inductance (mH/m)	1.94	1.67	1.67
b3	0.063	-0.003	-0.003
b5	0.171	0.008	-0.003
b7	0.061	0.012	-0.011
b9	-0.456	-0.255	-0.202
b11	0.180	0.232	0.156
b13	0.01	0.005	-0.001

Important characteristic of a cross-section is electromagnetic force applied to cable. Force component applied perpendicular to the cable wide side contributes to stress developed in the dipole midplane; that can be one of causes of cable degradation. On another hand, it is necessary to know this component to calculate needed prestress $\boldsymbol{P_{pr}}$:

$$P_{pr} \geq \frac{\sum_{1}^{N}(n \times F_n)}{N \times w},$$

where $\boldsymbol{N}$ is the number of turns per one layer, and $\boldsymbol{w}$ is cable width. It is easy to see that the pressure developed in the midplane due to Lorenz force

$$P_{L.F.} = \frac{1}{w} \times \sum_{1}^{N} F_n$$

is always larger then pressure developed during prestress.

Force component applied parallel to the cable wide side can lead to relative movement of strands in cable if corresponding stress exceeds friction or sheer strength. The sum of X-components of the force defines total confinement force needed to prevent the dipole from exploding. Table 3 summarizes force distribution for the three versions of the dipole cross-section design at quench level of central field.

Table 3

	#1		#2		#3	
	Inner layer	Outer layer	Inner layer	Outer layer	Inner layer	Outer layer
$\boldsymbol{P_{pr}}$, MPa	55.67	65.47	61.51	57.55	48.64	66.94
$\boldsymbol{P_{L.F.}}$, MPa	75.53	93.45	87.43	82.56	69.75	101.00
$\sum F_x$, MN/m	1.84	1.14	1.91	0.97	1.62	1.31

It is worth to notice that for the case #2 Lorenz force and needed prestress are larger for the inner layer. This can make this configuration interesting if stress in the inner layer is too high after preloading and cooling down.

Conclusion:

Several cross-sections were found attractive from the point of view of field quality, block arrangement, and magnet efficiency. Although they use the same cable, number of cables, number of blocks, and block pattern are different for these cross-sections. At least three of them can be candidates to choose from for the HFD model to build at FNAL. To help make a choice, numbers were obtained that summarize magnet properties for each of the three cross-section found. Besides these numbers, other criteria can/will be used for the final cross-section choice like availability of technological equipment, outer iron screen diameter, design stability to minor cross-section dimension changes, vacuum pipe and synchrotron radiation screen size, etc.

References:

1. S. Caspi, M. Wake
   A 12 Tesla Dipole for the VLHC
   LBNL Preprint SC-MAG-635, Berkeley, Dec. 16, 1998
2. M. Wake
   Conceptual Design of Nb_3Sn High Field Dipole Magnet
   KEK internal 98-3, July 1998
3. M. Wake
   Conceptual Design Update of Nb_3Sn High Field Dipole Magnet
   TD-99-009, FNAL, Oct. 1998
4. R. Yamada, M. Wake, and J. Moeller
   Design Study of 45mm Bore Dipole Magnet for 11 to 12 Tesla Field
   TD-99-012, FNAL, Mar. 1999
5. G. Ambrosio, V.V. Kashikhin
   40-mm Bore HFM Cross-Section design with 0.8 mm Strand Diameter Nb_3Sn Cable
   TD-99-010, FNAL, Mar. 99
6. E. Barzi
   I_C Degradation due to Cabling in Internal Tin Nb_3Sn
   TD-99-006, FNAL, Feb. 1999
7. T.T. Arkan, D.R. Chichili, and I. Terechkine
   Studies on S-2 Fiber Glass Insulation for Nb_3Sn Cable
   TD-98-063, FNAL, Nov. 1998
8. S. Russenchuck
   A Computer Program for the Design of Superconducting Accelerator Magnets
   CERN AT/95-39, LHC Note 354, Geneva, Switzerland, 26 Sept. 1995